LIMNOLOGY and OCEANOGRAPHY: METHODS

ASLO

Limnol. Oceanogr.: Methods 15, 2017, 867–874

doi: 10.1002/lom3.10205

Imaging FlowCytobot modified for high throughput by in-line acoustic focusing of sample particles

Robert J. Olson,[1] Alexi Shalapyonok,[1] Daniel J. Kalb,[2] Steven W. Graves,[2] Heidi M. Sosik *[1]

[1]Biology Department, Woods Hole Oceanographic Institution, Woods Hole, Massachusetts

[2]Center for Biomedical Engineering and Department of Chemical and Biological Engineering, The University of New Mexico, Albuquerque, New Mexico

Abstract

Imaging FlowCytobot, a submersible instrument that measures optical properties and captures images of nano- and microplankton-sized particles, has proved useful in plankton studies, but its sampling rate is limited by the ability of hydrodynamic focusing to accurately position flowing sample particles. We show that IFCB's sampling rate can be increased at least several-fold by implementing in-line acoustic focusing upstream of the flow cell. Particles are forced to the center of flow by acoustic standing waves created by a piezo-electric transducer bonded to the sample capillary and driven at the appropriate frequency. With the particles of interest confined to the center of the sample flow, the increased size of the sample core that accompanies increased sample flow rate no longer degrades image and signal quality as it otherwise would. Temperature affects the optimum frequency (through its effect on the speed of sound in water), so a relationship between sample temperature and optimum frequency for acoustic focusing was determined and utilized to control the transducer. The modified instrument's performance was evaluated through analyses of artificial particles, phytoplankton cultures, and natural seawater samples and through deployments in coastal waters. The results show that large cells, especially dinoflagellates, are acoustically focused extremely effectively (which could enable, for example, > 10-fold increased sampling rate of harmful algal bloom species, if smaller cells are ignored), while for nearly all cell types typically monitored by IFCB, threefold faster data accumulation was achieved without any compromises. Further increases are possible with more sophisticated software and/or a faster camera.

Imaging FlowCytobot (IFCB) is a submersible instrument that uses a combination of flow cytometric and video technology to capture high resolution (1 μm) images and to measure chlorophyll fluorescence of nano- and microplankton-sized particles (Olson and Sosik 2007). IFCB's images allow particles to be automatically classified (Sosik and Olson 2007), while the measurements of chlorophyll fluorescence allow discrimination between heterotrophic and phototrophic cells in taxa (such as dinoflagellates) that contain both kinds of members. IFCBs are typically deployed for 6 months with continuous sampling of 5 mL every 20 min, so that the observations made by IFCB can provide detailed information about the composition of the phytoplankton community over periods of hours to years (e.g., Sosik et al. 2010; Peacock et al. 2014; Brosnahan et al. 2016).

Since its original description, IFCB has been modified in several ways to improve its usefulness. The current instrument, which is commercially available (McLane Research Laboratories), is half as large and weighs half as much as the original, and requires a third of its power. These savings were accomplished by replacing off-the-shelf components used for convenience in the original instrument by custom-designed parts (syringe pump, signal processing and control boards, optical hardware) and by using new low-power versions of the computer and flash lamp. Laboratory versions of IFCB have been modified to enable studies of cells lacking chlorophyll fluorescence by automatically applying a fluorescent vital stain (Brownlee et al. 2016), to make it possible to assess DNA fluorescence and species-specific rRNA probe fluorescence in conjunction with images (Brosnahan et al. 2014), and to physically sort individual particles whose images have been captured (Lambert et al. 2016).

IFCB observations have revealed details of plankton dynamics including temporal and spatial variations in biomass and species composition (Sosik et al. 2010; Peacock et al. 2014; Brownlee et al. 2016), early warning for harmful algal blooms (Campbell et al. 2010, 2013), the importance of parasitism in

*Correspondence: hsosik@whoi.edu

the plankton (Brosnahan et al. 2014; Peacock et al. 2014), and insights into growth and life cycle transitions (Campbell et al. 2010; Brosnahan et al. 2016). These observations, while shedding new light on phytoplankton population dynamics, have also reinforced the fact that the plankton remains a paradox. Species come and go, some with regularity but others seemingly at random, and we still cannot predict or explain many of the patterns we observe. Is an unusual bloom or missing occurrence of a typical species caused by year-to-year differences in "seed" populations whose individuals are rare and thus inadequately sampled? Can we adequately detect and predict emerging blooms and, for the case of harmful taxa, do so early enough for effective response?

We describe here a new modification to IFCB, the addition of acoustic focusing, which allows IFCB to sample faster and thus to better address such questions.

IFCB's sampling rate is limited by the stringent requirements of imaging that allows cells to be resolved to genus or species level. The depth of focus of IFCB's microscope objective is only a few micrometers, so the cells must be confined within a sample core that is no thicker. To maximize the volume of sample water in the camera's focus, the flow cell channel is rectangular in cross section (860 $\times$ 180 μm), which causes the sample core to be hydrodynamically focused into a ribbon facing the camera. However, to achieve a core sufficiently thin that all cells are in focus, the sample flow rate must still be limited to about 0.25 mL min^{-1}. This sampling rate has proved sufficient (when combined with continuous operation) for many purposes, including early detection of harmful algal blooms (e.g., Campbell et al. 2013; Brosnahan et al. 2014), but for more detailed studies (including spatial surveys) even faster sampling is desirable.

Strategies to increase sampling rates

Increasing IFCB's sampling rate cannot be accomplished simply by increasing the pumping rate of sample, because this degrades the quality of the images. The size of the sample core is determined by the relative rates of sample flow and sheath flow; if the core gets thicker, some cells will no longer be at the proper distance from the objective. In addition, a wider core means that many cells will be outside the field of view of the camera. Increasing the sheath flow to correct the core thickness causes the velocity to increase and images to blur (i.e., movement of a cell by more than the 1-μm imaging resolution during the 1-μs flash exposure). An optical/mathematical approach to increase the depth of field exists (i.e., the wavefront coding system used in the commercial Amnis ImageStreamX fluorescence imaging flow cytometer, which allows spot counting throughout the depth of a cell), but in this approach the enhancement of depth-of-field comes at the expense of spatial resolution, and so it is not optimal for our aims.

An alternative approach to increase sampling rate is to pre-concentrate samples: remove most of the water from the sample, leaving the particles behind. Pre-concentration is a routine part of manual microscopic or bulk constituent analyses and is conventionally accomplished by settling, centrifugation, or filtration. The first two methods are not suitable for in situ operations, and the last is at best semi-quantitative when the samples need to be resuspended for analysis, as cells are destroyed and/or stick to filters.

Pre-concentration of particles can also be achieved through the use of acoustic standing waves (Goddard et al. 2006, 2007), a method that has been successfully incorporated into clinical flow cytometry in the Attune flow cytometer (Applied Biosystems). In situ environmental flow cytometry introduces additional demands and we have now adapted the approach to increase the sample throughput of an IFCB; we call the instrument so modified Imaging FlowCytobot-High Throughput (IFCB-HT).

Acoustic focusing

Acoustic waves exert force on suspended particles on the basis of differences in density and compressibility between particles and their surrounding fluid (Bruus 2012). When a cylindrical capillary is driven at the half-wavelength resonance frequency condition, a standing wave with a single pressure node radially focuses particles with positive contrast (denser and less compressible than the surrounding fluid) to the center of flow. Almost all biological cells in aqueous solutions move to nodes as they are denser and of equal (or lower) compressibility as compared to aqueous solutions. The force applied by acoustic standing waves scales with particle diameter and so becomes more effective as particle size increases, but acoustic focusing has been used with particles as small as a single bacteria ($\sim$ 1 μm diameter) (Lenshoff and Laurell 2010).

Though acoustic focusing devices can take several forms, among the simplest is a piezoelectric drive that generates a standing wave in a rigid cylindrical tube (Goddard et al. 2007; Ward et al. 2009). This approach has been applied to flow cytometry, where tests with plastic beads and mammalian cells showed that an acoustic system alone can achieve particle focusing comparable to that of a conventional hydrodynamic system. Furthermore, the combination of acoustic focusing and hydrodynamic focusing (Fig. 1, upper panel) has been shown to enhance the precision and sample delivery rates to flow cytometers (Ward et al. 2009).

Materials and procedures

IFCB modifications

The acoustic focusing element incorporated into IFCB comprised a piezoelectric transducer (Lead-Zirconate-Titanate, PZT) (1.5 MHz, 5 mm $\times$ 40 mm, APC International, Ltd.) bonded to a stainless steel capillary (Vici Valco T20C20–10, 1.5875 mm OD, 0.5 mm ID, 200 mm long) with a tapered nozzle end; this capillary served as the sample injection tube in IFCB (Fig. 1, lower panel). For bonding, the PZT was

attached via Superglue to a stainless steel plate (7 mm × 44 mm × 0.76 mm thick), which had been hard-soldered (45% Ag) to the capillary. The length of the modified injection tube required extending IFCB's frame and its watertight housing by 150 mm. The modifications to IFCB to create IFCB-HT increased the instrument's weight by ~ 5 kg, and the power required by ~ 5 W.

PZT control

Although the process is complex (Goddard and Kaduchak 2005), achievement of an acoustic standing wave with its node at the center of a capillary requires oscillating the PZT at a frequency related to the time required for sound waves to traverse the fluid and reflect back from the opposite wall; i.e., by the diameter of the capillary. Optimal focusing performance is achieved within a small bandwidth around this resonance frequency condition.

The PZT was supplied with oscillating (sine wave) DC power at user-defined amplitude (0–40 V) and frequency (1–2 MHz with 100 Hz resolution) by a custom-built programmable controller (DarklingX, LLC).

Since the speed of sound in water is affected by density, and thus by temperature, the temperature of the sample water in the capillary must be considered in calculating the optimal frequency for focusing. Density is also affected by salinity, but this effect is small enough (Kalb 2017) that it can be ignored for salinity changes on the order of 1 practical salinity unit (i.e., for most ocean sampling).

We were not able to measure directly the temperature of the water inside the capillary, so we measured the temperature of the outside of the capillary 2 cm upstream of the PZT (with a thermistor, 0.065″ diameter). We then used empirical calibrations to obtain a relationship between this temperature measurement and the frequency producing best focusing. Calibrations involved immersing the instrument and sample in a water bath and performing frequency scans at each of a range of water bath temperatures (Fig. 2). Frequency was increased (in 2 KHz steps) at 30 s intervals. During subsequent acoustic focusing operation, the relationship obtained from these calibrations (Fig. 3) was used to adjust the PZT frequency (typically at 30-s intervals) to maintain optimal focusing.

Assessment

We assessed the performance of IFCB-HT by comparing results of standard IFCB operation with those of faster flow and acoustic focusing. For comparison metrics we used distribution of positions of cells in the camera field, cell counting rate, and estimated cell concentration.

Cultured phytoplankton

In the laboratory, tests with phytoplankton cultures showed that large cells such as *Alexandrium tamarense* (30 μm dinoflagellate) are excellent subjects for acoustic focusing

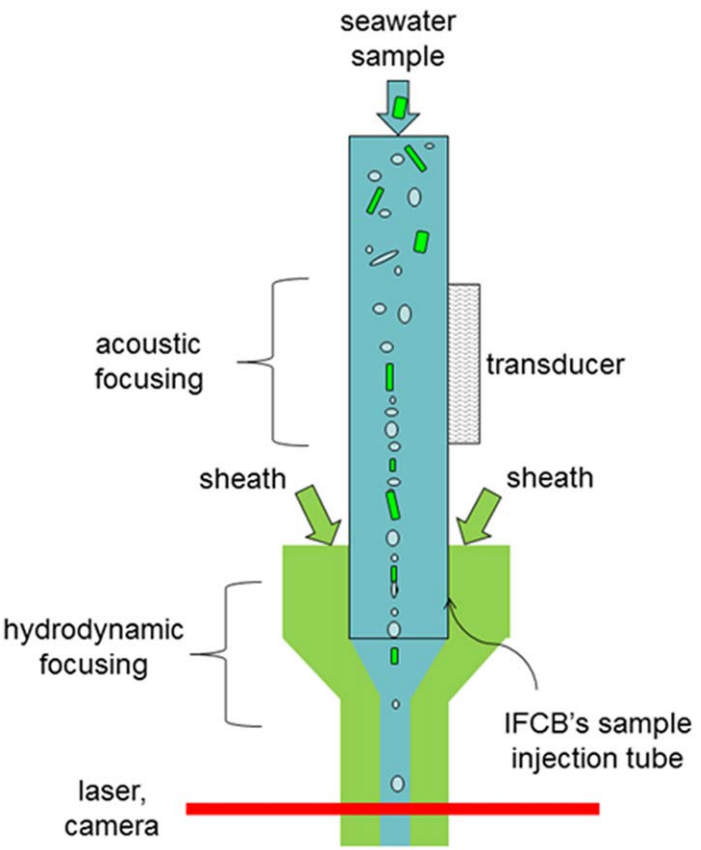

Fig. 1. (Upper panel) Schema of acoustic focusing as implemented in IFCB (not to scale). A piezoelectric transducer mounted to the sample injection tube (*see* Lower panel) generates acoustic standing waves that force particles to the center of the flow (when driven by electric current pulsating at the correct frequency). Since only the center of the sample flow now contains the particles of interest, the increasing size of the sample core that comes with higher sample flow rate no longer degrades image and signal quality as it normally would. (Lower panel) PZT-capillary assembly developed for use in IFCB. The ceramic Lead Zirconate Titanate (PZT) transducer is superglued to a stainless steel plate that has been silver-soldered to a stainless steel capillary, which serves as IFCB's sample injection tube. A thermistor measures temperature of the capillary.

(Fig. 4; Kalb 2017). Cells of this species were confined to the center of the channel even at 5 mL min^{-1} (20 times the normal sample rate). The number of cells observed in a given time was increased in the fast runs, though by less than the nominal factor. This is because new triggers are blocked during image processing, causing some of the sample to pass unexamined; since processing time (which is monitored and

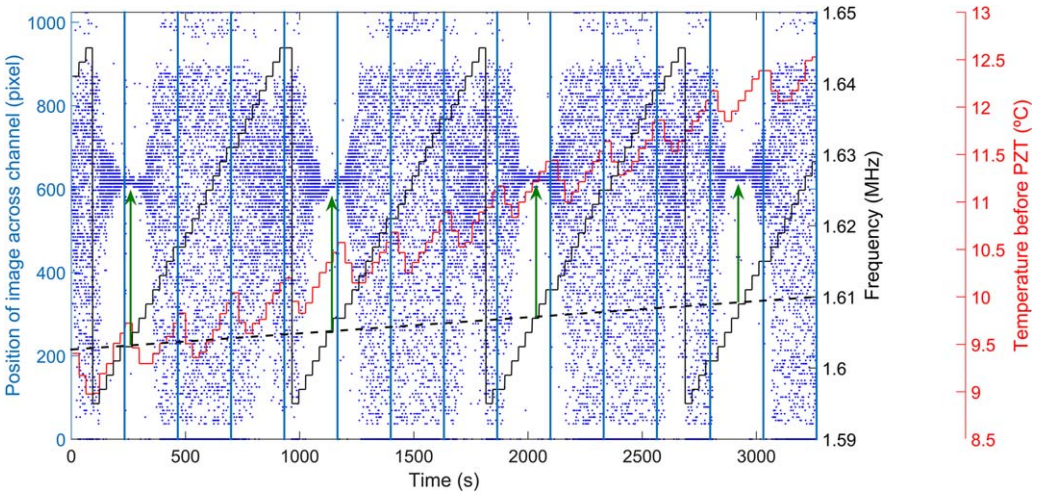

Fig. 2. To identify the optimum frequency for acoustic focusing as a function of water temperature, IFCB-HT was immersed in a water bath and 10-mL samples of 9 μm beads were repeatedly analyzed at 2.5 mL min^{-1}. Each blue dot represents the position of a bead image across the flow cell channel, with pixels 0 and 1024 being the edges of the camera field of view. As the water bath temperature (red) changed (total range 8–32°C), PZT frequency was repeatedly scanned with increases of 2 KHz at 30-s intervals (black stepped line). When acoustic focusing occurred, the beads were forced to the center of the channel (*see* arrows, with dashed line indicating how the frequency producing optimum focusing changed with temperature). The distributions of image positions in the camera field of view revealed that, in the temperature range shown here, the best acoustic focusing occurred at ~ 1.61 MHz, and that the optimum frequency increased with temperature. Vertical blue lines indicate transitions between 10-mL samples. Temperature increases are observed during each analysis because the instrument interior is ~ 7°C warmer than the surrounding water and thus each new sample warms during analysis; and to a lesser extent because of heat produced by the PZT during acoustic focusing.

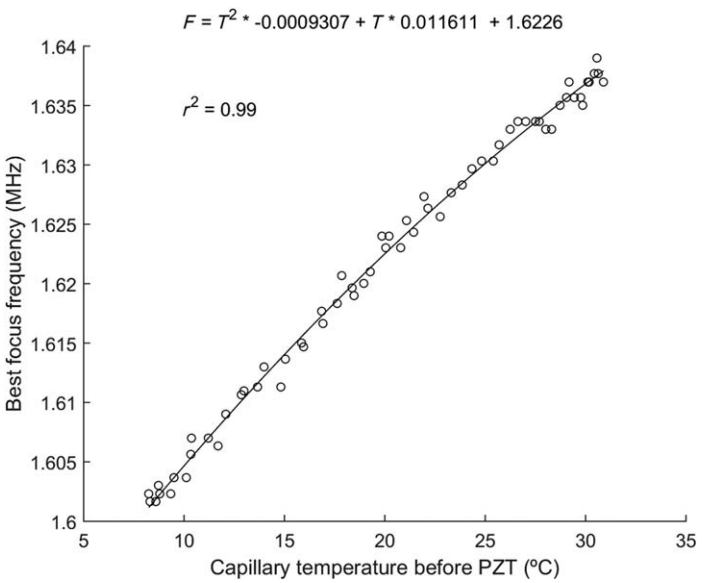

Fig. 3. Frequency scans at different temperatures (*see* Fig. 2) were used to derive a relationship between optimal PZT frequency for focusing and temperature. A 2nd degree polynomial was fit to the data.

considered when calculating the volume of water analyzed) is nearly a constant, the fraction of sample ignored increases with the trigger rate.

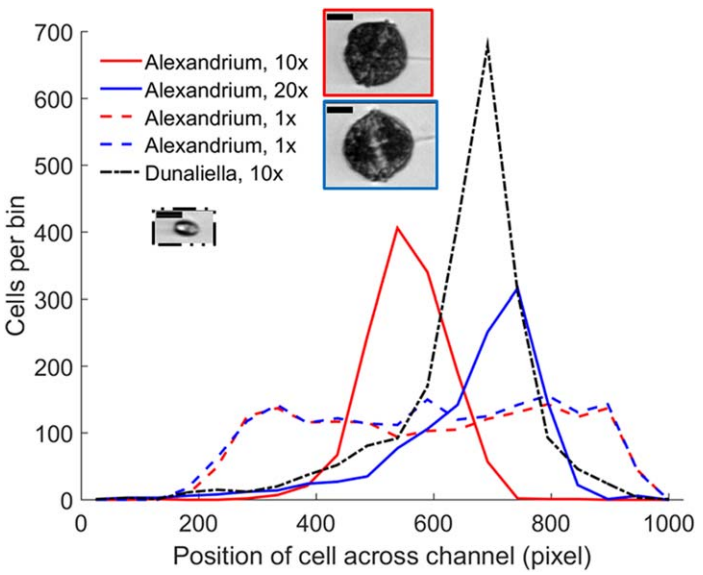

Fig. 4. Acoustic focusing of cultured phytoplankton cells was assessed by examining the positions of cells across the flow cell channel. *A. tamarense* cells were analyzed using IFCB-HT in the laboratory at three sampling rates: normal IFCB operation (1× = 0.25 mL min^{-1}), and with acoustic focusing at 10× and 20× the normal rate. In a separate measurement, cultured *D. tertiolecta* cells were analyzed with acoustic focusing at 10× the normal rate. Line colors and styles in the borders around the example cell images correspond to those in the legend; scale bars are 10 μm.

Acoustic focusing efficiency generally scales with cell size, but we found that *Dunaliella tertiolecta*, an 8-μm chlorophyte, could be focused effectively at 2.5 mL min^{-1} (Fig. 4). Coincidentally, these cells are also near the lower size limit for useful imaging by IFCB; few cells below this size range are taxonomically distinct in IFCB images. Cultured *Synechococcus* cells, which at $\sim$ 1 μm are just visible in IFCB images (though with fluorescence too low to trigger), were not acoustically focused by IFCB-HT even when run at 0.025 mL min^{-1} (10$\times$ slower than normal; not shown).

Field trials

We deployed an early version of IFCB-HT for 2 weeks during a bloom of the toxic dinoflagellate *A. tamarense* in Salt Pond (Nauset, Massachusetts); these results will be presented elsewhere (Brosnahan et al., unpubl.). At other times during the same bloom, water samples were analyzed with IFCB-HT in the laboratory (Fig. 5).

Evaluation of acoustic focusing of a wide variety of cell types was carried out during a deployment in Woods Hole Harbor, Massachusetts, in which the instrument was programmed to alternate between equal durations of conventional operation (1 mL sample at 0.25 mL min^{-1}) and acoustic focusing with 10-fold increased sample rate (10 mL sample at 2.5 mL min^{-1}). For a 12-h period during this deployment, representative cell types were classified from their images (by a combination of automated analysis and manual verification) and their positions in the camera field of view were determined (Fig. 6). The results show that a 10-fold increase in sampling rate was practical for nearly all of the particles of interest. Dinoflagellates (including *Alexandrium*, Fig. 5) were very strongly focused, as were cells of the genus *Dictyocha* (Fig. 6A), presumably because of their relatively large size and lack of large vacuoles. The large solitary diatoms from the genera *Pleurosigma*, *Rhizosolenia*, and *Ditylum* were also effectively focused, as was *Guinardia delicatula*, a large-celled species forming straight chains. At least some types of detritus were also strongly focused.

A second group of cell types were somewhat less effectively focused, with some cells outside the center of the camera's field of view, though very few were near the edges. This group included small cells (the diatom *Cerataulina pelagica* and cryptophytes) and large diatoms that formed three-dimensional colonies (e.g., *Guinardia striata*, *Asterionellopsis glacialis*, and *Thalassionema* spp.) (Fig. 6B). The effects of the acoustic forcing, which decreases as it approaches the node in the center of flow (Kalb 2017) probably differ within a large colony, depending on its orientation, and large colonies could also be affected by the difference in velocity between the center and edges of flow. However, it is worth noting that tight acoustic focusing is less critical for these large colonies because they are often thicker than the system's depth of focus (so that some parts are in optical focus and some not), and colony-forming species can often be identified even if part of the colony is out of the field of view.

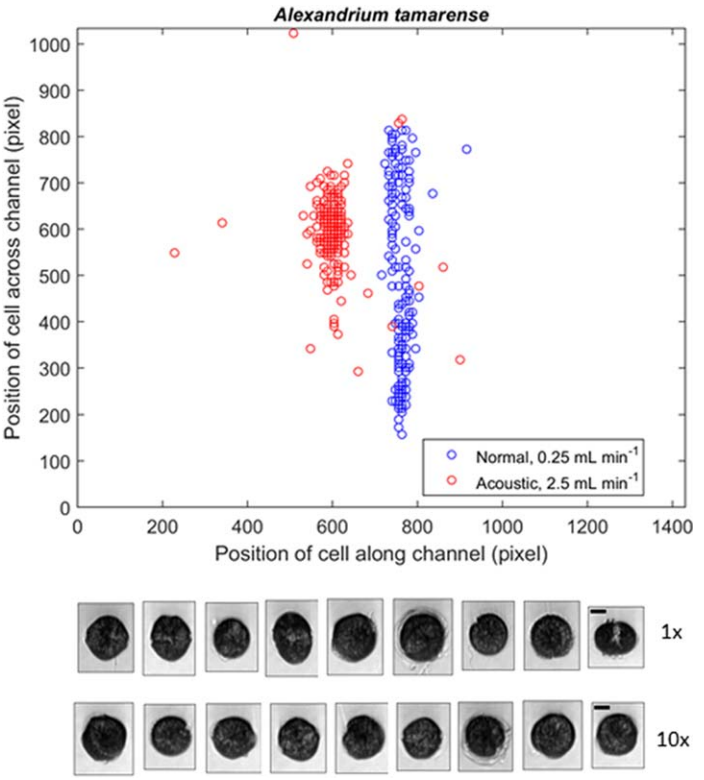

Fig. 5. (Upper panel) Water samples from Salt Pond during a bloom were analyzed with IFCB-HT in the laboratory at the normal rate without acoustic focusing (image positions indicated by blue symbols) and at 10-fold higher rates with acoustic focusing (red). *A. tamarense* cells, as identified by an automated classifier, were more tightly constrained in the camera's field of view by acoustic focusing, even at high rates, than in normal operation, suggesting that these cells could be successfully analyzed at even higher sampling rates. (Lower panel) Representative images from the two analyses; scale bars are 10 μm.

Another group of cells for which acoustic focusing allowed acceptable performance at 10-fold increased sampling rate were the ciliate genera *Strombidium*, *Laboea*, and *Mesodinium* (Fig. 6C). It is possible that these cells are actually well focused acoustically, since they appear similar in size and composition to some of the cells in Fig. 6A, but that their motility enables some of them to begin to "escape" from the center of flow before imaging. This possibility could be investigated with immobilized cultures of *Mesodinium*.

Cells in the diatom genus *Leptocylindrus*, which are only $\sim$ 2 μm wide, are apparently too small for quantitative operation at 10-fold normal sampling rate even with acoustic focusing (Fig. 6D); these cells formed a broad band across the field of view. Many unidentified small ciliates were focused relatively tightly, but some were located near the edges of the field of view; this may reflect the combination of their small size and motility. The large-celled diatom *Guinardia flaccida* showed a very broad distribution, but this could be at least partly related to long chains "flipping" during flow rather than to a lack of acoustic focusing. Some images show chains at large angles to the flow axis,

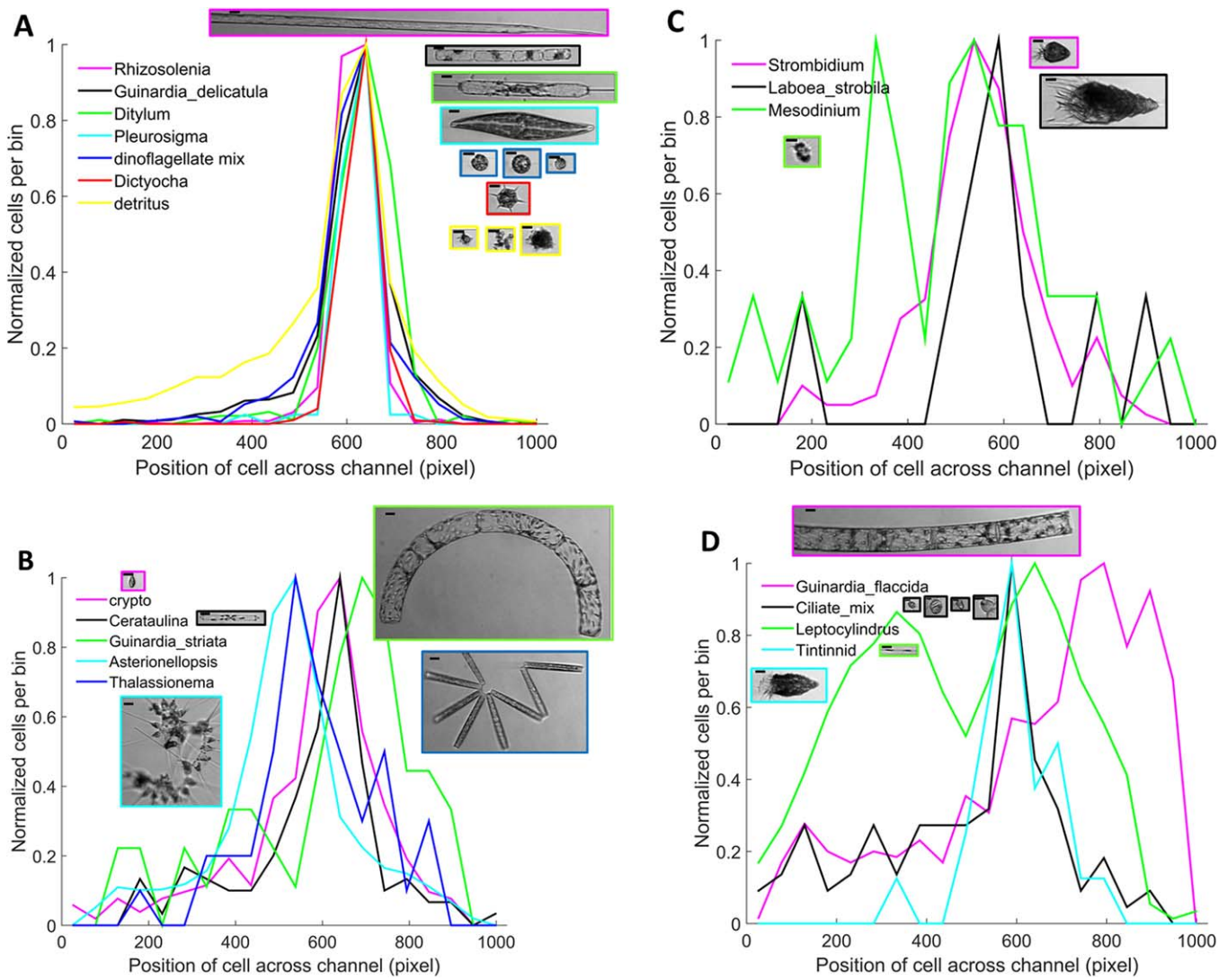

Fig. 6. Distributions of image positions in the camera's field of view during fast sampling (10× normal) with acoustic focusing. Scale bars in image examples are 10 μm. The across-channel positions were grouped into 20 equal-width bins, and frequencies normalized to the total number of cells in each category. Line colors in the borders around the example cell images correspond to those in the legends. Particle categories in A, B, C, and D were acoustically focused with decreasing efficiencies.

including some that spanned the entire camera field (in the cross-channel dimension), rather than being aligned to the flow axis; this phenomenon occurred more frequently (up to ~ 10% of images) at 10× than at normal sampling rate, and is likely caused by the effect of the non-uniform cross-channel velocity profile (i.e., lower velocity near channel walls) on off-center chains.

Overall, cell concentrations derived from 10-fold faster sampling with acoustic focusing were similar to those from normal IFCB operation (Fig. 7), as expected since the same water was being sampled in both cases and our approach quantitatively accounts for the higher sample volume analyzed with acoustic focusing. The number of cells observed and corresponding sample volume were ~ 3-fold higher for the acoustically focused analyses, so the confidence intervals around their concentration estimates (assuming Poisson-distributed observations) were narrower.

Even though sample water was introduced 10-fold faster, the increase in cells observed was only threefold. This is due to the fact that processing time (during which no new triggers can be acquired) is a larger fraction of the running time for the 10× samples, simply because triggers occur more frequently. This effect could have been lessened by increasing the trigger threshold to sample only large, rare cells (thereby reducing the trigger rate), but for the purposes of this evaluation (comparison of sampling rates) we did not do this.

For two cell types, estimated cell concentrations were higher from 1× than from 10× sampling rates: *Leptocylindrus* spp. (category 10 in Fig. 7) and tintinnids (category 16 in

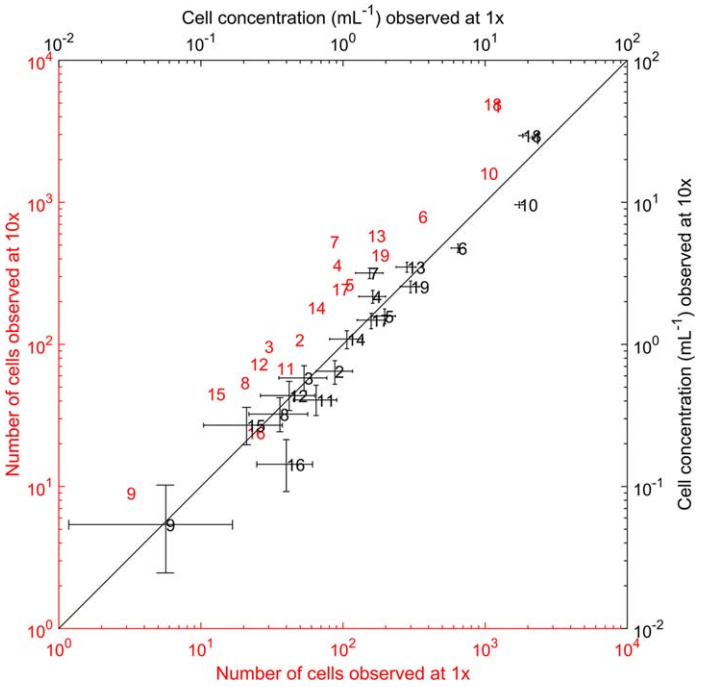

Fig. 7. Numbers of cells observed (red) and cell concentrations (black) from 12 h of an IFCB-HT deployment in Woods Hole Harbor, for representative classes identified from images (1 = *A. glacialis*; 2 = *C. pelagica*; 3 = miscellaneous ciliates; 4 = *Dictyocha* spp.; 5 = *Ditylum brightwellii*; 6 = *G. delicatula*; 7 = *G. flaccida*; 8 = *G. striata*; 9 = *Laboea strobili*; 10 = *Leptocylindrus* spp.; 11 = *Mesodinium* spp.; 12 = *Pleurosigma* spp.; 13 = *Rhizosolenia* spp.; 14 = *Strombidium* spp.; 15 = *Thalassionema*; 16 = tintinnids; 17 = cryptophytes; 18 = detritus; 19 = dinoflagellates). Instrument operation alternated between normal IFCB sampling ("1×," 0.25 mL min^{-1}) and sampling with acoustic focusing ("10×," 2.5 mL min^{-1}), for equal durations (4 min per sample). The diagonal black line is 1 : 1. Error bars represent 95% confidence intervals for cell concentrations derived assuming Poisson-distributed observations.

Fig. 7). *Leptocylindrus* was not acoustically focused well (as shown in Fig. 6D), probably due to its small size, so a significant number of these cells were not imaged (they passed outside the camera's field of view). Tintinnids, in contrast, appeared to acoustically focus adequately (Fig. 6D), but the number of cells observed in the 10× samples was almost the same as that from 1× samples, and thus the cell concentration estimates from 1× sampling were higher than from 10× sampling ($p = 0.001$). We speculate that some cells were destroyed by increased shear at the higher flow rate or by heating that accompanies acoustic focusing. The opposite situation occurred for *G. flaccida* (category 7 in Fig. 7): the cell concentration estimated from 10× sampling was significantly higher than from 1× sampling ($p < 0.001$). We speculate that at low flow rate some of these very large chains may not make it through the sampling tubing, but at the higher flow rate they are more effectively carried along.

Both kinds of deviations from the commonly observed pattern require further investigation.

Discussion

Our results demonstrate that with relatively minor modification to IFCB its sampling rate can be increased at least several fold, providing data more quickly and/or with better precision. This improvement will be important for many plankton studies: it will enable surveys to obtain finer spatial-scale data and moored instruments to measure lower concentrations of target species (e.g., to improve early detection of harmful algal blooms), and will facilitate operation at locations with limited power by allowing shorter duty cycles. In our Woods Hole Harbor demonstration, acoustic focusing only allowed measurement of ~ 3 times more cells than standard IFCB operation, because we used stringent conditions for the comparison holding all other operating parameters identical. For practical operation in cases such as sampling of many harmful algal bloom species, closer to 10-fold faster counting will be readily possible by raising the fluorescence threshold to avoid triggering on smaller cells that typically dominate.

Good acoustic focusing of some cell types (notably *Alexandrium*) has been observed at rates as high as 40× (data not shown), but such rates are not yet practical for routine use. For example, at very high sampling rates, precise centering of the sample capillary becomes critical, and even though IFCB's camera is capable of 30 frames per second, the current IFCB software and computing hardware limits its processing rate to about 12 frames per second. Imaging speed could be improved by parallel processing and multi-thread programming (to take advantage of potential processing time now spent idle while new sample is being drawn, tubing rinsed, etc.); ultimately a faster camera could also be used. Since faster sampling has been demonstrated, it becomes important to explore these avenues.

The modifications described here, which we estimate to cost $10,000 (mostly for the longer pressure vessel), increased throughput (rate of observations) by a factor of three without any optimization of trigger threshold for high sampling rates; this applied to almost all the cell types we encountered in our coastal field testing. For specialized applications, such as detection of dinoflagellate blooms, considerably better results can be obtained (at the cost of missing small cells). We envision most applications to involve alternation between normal sampling rate and higher rates with acoustic focusing. Normal sampling will quantify small cells (usually numerous), and even a limited number of large cells sampled will provide an internal check on the efficacy of higher sampling rates with acoustic focusing (as in Fig. 7).

Comments and recommendation

At least for initial applications of IFCB-HT, we recommend alternating between fast sampling with acoustic focusing and normal IFCB operation, to determine the maximum sampling rate that produces quality data for new cell types of interest, and to optimize trigger threshold settings for

high sampling rates. At present, the most advantageous application of IFCB-HT would appear to be in studies of harmful dinoflagellate blooms.

In view of the apparent undersampling of tintinnid cells during fast sampling (compared to normal sampling), as well as the higher-than-expected results for very large diatom chains (which may imply that normal operation undersamples these cells), we recommend that studies focusing on particular species include initial comparisons of IFCB counts with microscopic or other independent estimates of abundance. The wide variety of cell types in the plankton makes it difficult to foresee all their responses.

The effect of salinity on the optimum frequency for acoustic focusing (through water density) is expected to become significant when sample salinity varies by >1 P.S.U. (as, for example, in estuaries). It should be straightforward to employ an empirical calibration (similar to that described above for temperature, but using an external salinity sensor to measure the salinity of sample water) to deal with this issue.

References

Brosnahan, M. L., S. Farzon, B. Keafer, H. M. Sosik, R. J. Olson, and D. M. Anderson. 2014. Complexities of bloom dynamics in the toxic dinoflagellate *Alexandrium fundyense* revealed through DNA measurements by imaging flow cytometry coupled with species-specific rRNA probes. Deep-Sea Res. II **103**: 185–198. doi:10.1016/j.dsr2.2013.05.034

Brosnahan, M. L., and others. 2016. Rapid growth and concerted sexual transitions by a bloom of the harmful dinoflagellate *Alexandrium fundyense* (Dinophyceae). Limnol. Oceanogr. **6**: 2059–2078. doi:10.1002/lno.10155

Brownlee, E. F., R. J. Olson, and H. M. Sosik. 2016. Microzooplankton community structure investigated with imaging flow cytometry and automated live-cell staining. Mar. Ecol. Prog. Ser. **550**: 65–81. doi:10.3354/meps11687

Bruus, H. 2012. Acoustofluidics 7: The acoustic radiation force on small particles. Lab Chip **12**: 1014–1021. doi:10.1039/c2lc21068a

Campbell, L., R. J. Olson, H. M. Sosik, A. Abraham, D. W. Henrichs, C. J. Hyatt, and E. J. Buskey. 2010. First harmful *Dinophysis* (Dinophyceae, Dinophysiales) bloom in the U.S. is revealed by automated imaging flow cytometry. J. Phycol. **46**: 66–75. doi:10.1111/j.1529-8817.2009.00791.x

Campbell, L., D. W. Henrichs, R. J. Olson, and H. M. Sosik. 2013. Continuous automated imaging-in-flow cytometry for detection and early warning of *Karenia brevis* blooms in the Gulf of Mexico. Environ. Sci. Pollut. Res. **20**: 6896–6902. doi:10.1007/s11356-012-1437-4

Goddard, G., and G. Kaduchak. 2005. Ultrasonic particle concentration in a line-driven cylindrical tube. J. Acoust. Soc. Am. **117**: 3440–3447. doi:10.1121/1.1904405

Goddard, G., J. C. Martin, S. W. Graves, and G. Kaduchak. 2006. Ultrasonic particle-concentration for sheathless focusing of particles for analysis in a flow cytometer. Cytometry Part A **69A**: 66–74. doi:10.1002/cyto.a.20205

Goddard, G. R., C. K. Sanders, J. C. Martin, G. Kaduchak, and S. W. Graves. 2007. Analytical performance of an ultrasonic particle focusing flow cytometer. Anal. Chem. **79**: 8740–8746. doi:10.1021/ac071402t

Kalb, D. M. 2017. High throughput acoustic focusing for separation and interrogation of biological particles. Ph.D. thesis. Univ. of New Mexico.

Lambert, B. S., R. J. Olson, and H. M. Sosik. 2016. A fluorescence-activated cell sorting subsystem for the Imaging FlowCytobot. Limnol. Oceanogr.: Methods **15**: 94–102. doi:10.1002/lom3.10145

Lenshoff, A., and T. Laurell. 2010. Continuous separation of cells and particles in microfluidic systems. Chem. Soc. Rev. **39**: 1203–1217. doi:10.1039/b915999c

Olson, R. J., and H. M. Sosik. 2007. A submersible imaging-in-flow instrument to analyze nano- and microplankton: Imaging FlowCytobot. Limnol. Oceanogr.: Methods **5**: 195–203. doi:10.4319/lom.2007.5.195

Peacock, E. E., R. J. Olson, and H. M. Sosik. 2014. Parasitic infection of the diatom *Guinardia delicatula*, a recurrent and ecologically important phenomenon on the New England Shelf. Mar. Ecol. Prog. Ser. **503**: 1–10. doi:10.3354/meps10784

Sosik, H. M., and R. J. Olson. 2007. Automated taxonomic classification of phytoplankton sampled with imaging-in-flow cytometry. Limnol. Oceanogr.: Methods **5**: 204–216. doi:10.4319/lom.2007.5.204

Sosik, H. M., R. J. Olson, and E. V. Armbrust. 2010. Flow cytometry in phytoplankton research, p. 171–185. In D. J. Suggett, O. Prasil, and M. A. Borowitzka [eds.], Chlorophyll a fluorescence in aquatic sciences: Methods and applications. Developments in applied phycology 4. Springer.

Ward, M., P. Turner, M. DeJohn, and G. Kaduchak. 2009. Fundamentals of acoustic cytometry. Curr. Protoc. Cytom. **49**: 1.22.21–21.22.12. doi:10.1002/0471142956.cy0122s49

Acknowledgments

We would like to thank E. Crockford and E. Peacock for technical assistance and E. Olson for suggesting silver-solder for a durable bond between the PZT and the sample injection needle. This research was supported by grants from the NSF (OCE-1130140 and OCE-1131134).

Conflict of Interest

None declared.

Submitted 17 May 2017
Revised 1 August 2017
Accepted 14 August 2017

Associate editor: Malinda Sutor